Surgical and Radiologic Anatomy (2023) 45:149–157
https://doi.org/10.1007/s00276-022-03075-7

ORIGINAL ARTICLE

Delineation of the lacrimal vein: a magnetic resonance imaging study

Satoshi Tsutsumi[1] · Natsuki Sugiyama[1] · Hideaki Ueno[1] · Hisato Ishii[1]

Received: 14 November 2022 / Accepted: 29 December 2022 / Published online: 3 January 2023

Abstract

Purpose To our knowledge, anatomical knowledge about the lacrimal vein (LV) is missed. Therefore, this retrospective study aimed to explore them using magnetic resonance imaging (MRI).

Materials and methods Eighty-one patients who underwent contrast-enhanced MRI and three donated bodies to science were enrolled.

Results On the sagittal images, the measured mean right long (LD) and short diameters (SD) of the lacrimal gland (LG) were 17.3 ± 2.4 mm and 13.7 ± 2.1 mm, while the left LD and SD were 17.0 ± 2.6 mm and 13.6 ± 2.6 mm, respectively. Laterality or sex differences were not found in the LD and SD groups. In addition, no specific age range was associated with a significantly longer LD or SD. LVs were identified in 94% of axial images. Their course was classified into as follows: three types: connecting to the superolateral cavernous sinus (CS), to the superior ophthalmic vein (SOV), and the diploic channels of the greater wing of the sphenoid bone (DCGW). The CS type was the most frequently identified, followed by the SOV and DCGW types. In dissected specimens, the LVs consistently coursed between the posterior margin of the LG and the superolateral part of the CS, above the upper margin of the lateral rectus muscle.

Conclusions The LV may consistently emerge from the upper posterior margin of the LG. It commonly pours into the SOV or superolateral part of the CS.

Keywords Lacrimal gland · Lacrimal vein · Anatomy · Orbit · Magnetic resonance imaging

Introduction

The lacrimal gland (LG) is known to be a flat orbital structure that produces tears. The acinar portion of the LG is thought to derive from the neuroectoderm [25]. It is superficially located in the lacrimal fossa, a shallow cavity in the superolateral corner of the orbit, and adjacent to the bulb [20]. The LG can be exposed through a lateral orbitotomy [1, 8]. A recent investigation suggested that normal LG—commonly comprising the orbital and palpebral lobes—may exhibit morphological and histological variations [15, 17]. Extensive studies on donated bodies to science, magnetic resonance imaging (MRI), computed tomography (CT), and Doppler sonography have explored normal LGs [2, 4–6, 9, 14, 15, 17–19, 21, 23–27]. On contrast-enhanced MRI, the LG is delineated as an enhancing area [18, 24]. Lesions of the LG fossa involve diverse pathologies, including inflammation, autoimmune diseases, lymphoproliferative disorders, benign epithelial proliferation, malignant neoplasia, and metastatic disease [12, 22]. Abnormal LG enlargements have been associated with Sjögren's syndrome, IgG4-related diseases, acromegaly, Graves' ophthalmopathy, sickle cell disease, and lymphoblastic leukemia [3, 7, 10, 11, 13, 16, 28].

In contrast to investigations of the lacrimal artery (LA), to our knowledge, we miss clear depiction and MRI aspects of the lacrimal vein (LV) [5, 6, 26]. Therefore, the present study aimed to explore the LV and its relationship with the LG using thin-slice contrast-enhanced MRI.

Materials and methods

This retrospective study included 81 outpatients who underwent MRI examinations after presentation to our hospital between July 2010 and May 2015. These patients presented

✉ Satoshi Tsutsumi
shotaro@juntendo-urayasu.jp

[1] Department of Neurological Surgery, Juntendo University Urayasu Hospital, 2-1-1 Tomioka, Urayasu, Chiba 279-0021, Japan

with headaches, dizziness, tinnitus, hearing disturbances, hemisensory disturbances, gait disturbances, scintillation scotoma, and focal seizures. The patient population comprised 39 men and 42 women, with a mean age of 51.1 ± 15.5 years (range, 18–78 years). Patients with a medical history of dry eye, collagen disease, or thyroid orbitopathy were excluded. Initial examinations using axial T1- and T2-weighted sequences, T2-gradient echo, fluid-attenuated inversion recovery, and diffusion-weighted sequences confirmed that the absence of intracranial or intraorbital tumors, cavernous sinus (CS) lesions, symptomatic ventriculomegaly, or traumatic orbital injuries. Subsequently, the patients underwent thin-sliced, volumetric imaging examination with intravenous gadolinium infusion (0.1 mmol/kg) in the axial, coronal, and strictly sagittal planes, involving the entire cranial vault. The following parameters were adopted: repetition time, 4.1 ms; echo time, 1.92 ms; slice thickness, 1 mm; interslice gap, 0 mm; matrix, 320 × 320; field of view, 250 mm; flip angle, 13°; and scan duration, 7 min 25 s. All images were obtained using a 3.0-T MR scanner (Achieva R2.6; Philips Medical Systems, Best, The Netherlands). Imaging data were transferred to a workstation (Virtual Place Lexus 64. 64th edition; AZE, Tokyo, Japan) and independently analyzed by two authors (S.T. and H.I., both of whom had more than 15 years of experience as board-certified neurosurgeons). The LGs and LVs were assessed on the contrast-enhanced axial and sagittal images. On sagittal images, an enhancing, oval or round structure located adjacent to the superolateral surface of the bulb was regarded as the LG. The long (LD) and short diameters (SD) of the LG were measured on a sagittal image, which revealed the largest dimension (Fig. 1). Furthermore, linear intensities

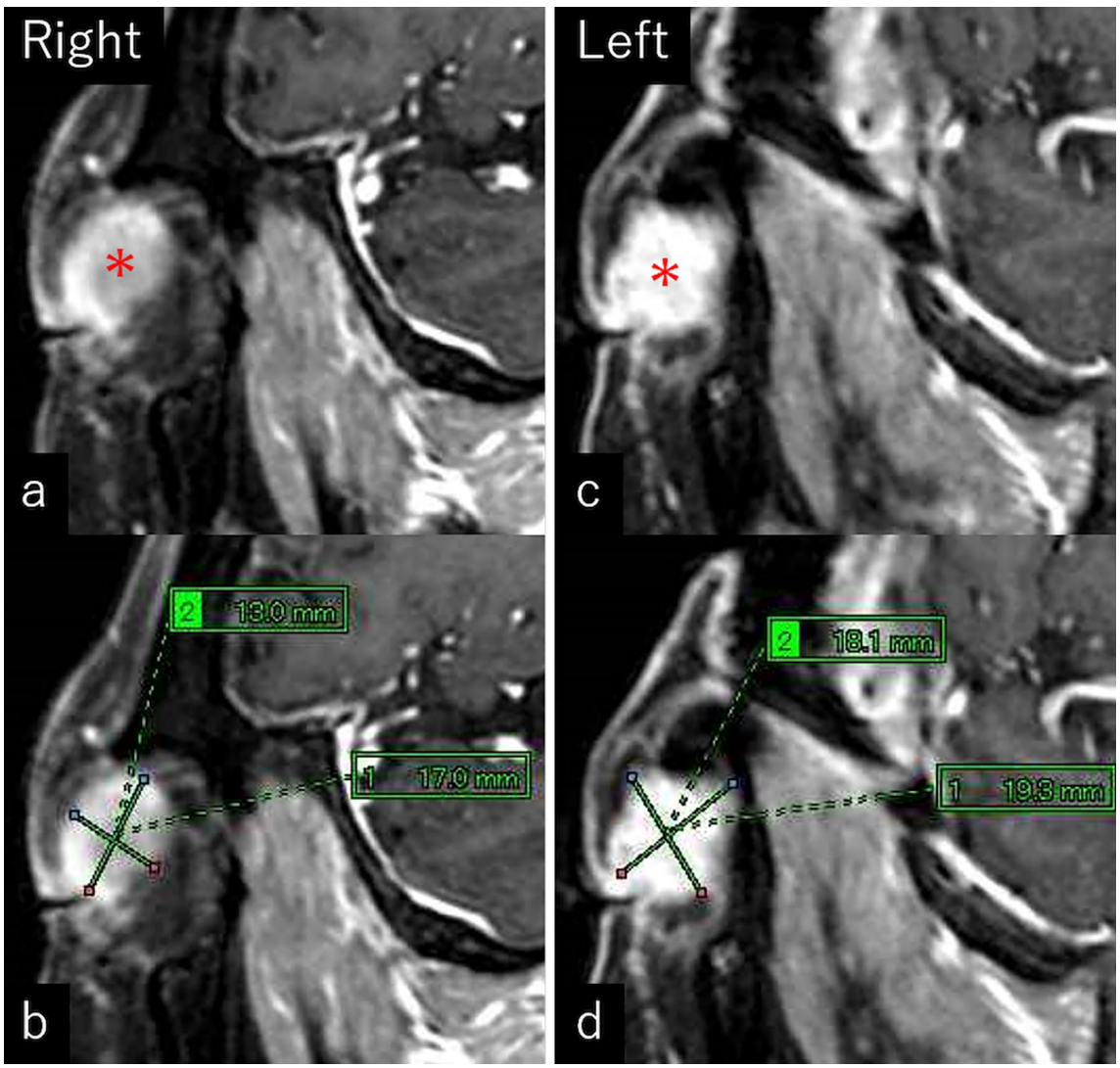

Fig. 1 Contrast-enhanced sagittal magnetic resonance images showing measurements of the long (**b** ,**d**, 1) and short (**b**, **d**, 2) diameters of the lacrimal glands (**a**, **c**, asterisk) bilaterally

Table 1 Measured mean diameters of the lacrimal glands

	LD (mm)	SD (mm)
Right	17.3 ± 2.4 (12.2–24.1)	13.7±2.1 (6.2–18.6)
Left	17.0 ± 2.6 (12.0–23.4)	13.6±2.6 (6.7–24.6)

LD long diameter, *SD* short diameter

Table 2 Laterality and sex difference in measured diameters

	Diameter	Result
Laterality	LD	NS ($P > 0.05$)
	SD	NS ($P > 0.05$)
Sex difference	LD, right	NS ($P > 0.05$)
	SD, right	NS ($P > 0.05$)
	LD, left	NS ($P > 0.05$)
	SD, left	NS ($P > 0.05$)

LD long diameter, *NS* not significant, *SD* short diameter

connecting the LG to other intraorbital or intracranial venous structures were considered LVs. Because of their low performance in depicting LVs, as confirmed via preliminary observations, coronal images were not used.

The Wilcoxon signed-rank test was used for the statistical analyses. Differences were considered statistically insignificant at $p > 0.05$.

Furthermore, the LGs and LVs were observed on three dissected donated bodies for science where the bilateral internal jugular veins were manually injected with blue coloring liquid. In two bodies, relationships between the LV and relevant structures were observed in four orbits. In the remaining body, a lateral orbitotomy was performed bilaterally to explore the sagittal dimension of the LG and LV. Dissections were performed by one author (S.T.) at the Department of Neurological Surgery, University of Florida, Gainesville, FL, USA.

This study was conducted in accordance with the guidelines of our institution for Human Research. Written informed consent was obtained from all patients prior to their participation.

Results

Contrast-enhanced MRI examinations

The LGs were consistently delineated bilaterally in all 81 patients, with variable enhancements. On the sagittal images, the mean right LD and SD were measured 17.3 ± 2.4 mm (range: 12.2–24.1) and 13.7 ± 2.1 mm (6.2–18.6), while the left LD and SD were 17.0±2.6 mm (12.0–23.4) and 13.6 ± 2.6 mm (6.7–24.6), respectively (Table 1). Laterality was not observed in the LD or SD groups ($p > 0.05$). Bilaterally, no sex difference was observed in the LD or SD (Table 2). Furthermore, no specific age range in 10-year increments was associated with a significantly longer LD or SD ($p > 0.05$). In the sagittal images, two or more vascular structures arose from the superoposterior margin of the LGs. They were identified in 24 of 81 patients (30%), with 9 on the right, 9 on the left, and 6 on both sides (Fig. 2). Due to the low performance in depicting more posterior courses, these vessels were not identified as LVs or LAs. On axial images, the LV was identified in 76 patients (94%). Their course was classified into three types: connecting to the superolateral CS, connecting to the superior ophthalmic vein (SOV), and connecting to the diploic channels of the greater wing of the sphenoid bone (DCGW) (Fig. 3). The CS type was the most frequent and found in 47 of 76 identified patients (62%), with 8 on the right, 5 on the left, and 34 on both sides. The SOV type comprised 22 patients (29%), with 10 on the right, 6 on the left, and 6 on both sides. The DCGW type was the least frequent and observed in 7 (9%) patients, with 0 on the right, 1 on the left, and 6 on both sides (Table 3). The CS, SOV, and DCGW types exhibited highly variable morphologies (Fig. 4).

Donated bodies to science

On dissected specimens, the LVs were consistently coursed between the posterior margin of the LG and the superolateral part of the CS, above the upper margin of the lateral rectus muscle (Fig. 5). Connections between the LV and the SOV were not observed in dissected specimens. When viewed through the lateral orbitotomy, all identified LVs emerged from the posterior margin of the LG and coursed posteriorly along the course of the LAs (Fig. 6).

Discussion

In the present study, the identified LVs on MRIs consistently emerged from the upper posterior margin of the LGs, coursed posteriorly, and drained into the superolateral CS, SOV, and DCGW. Presurgical evaluation of accurate LV

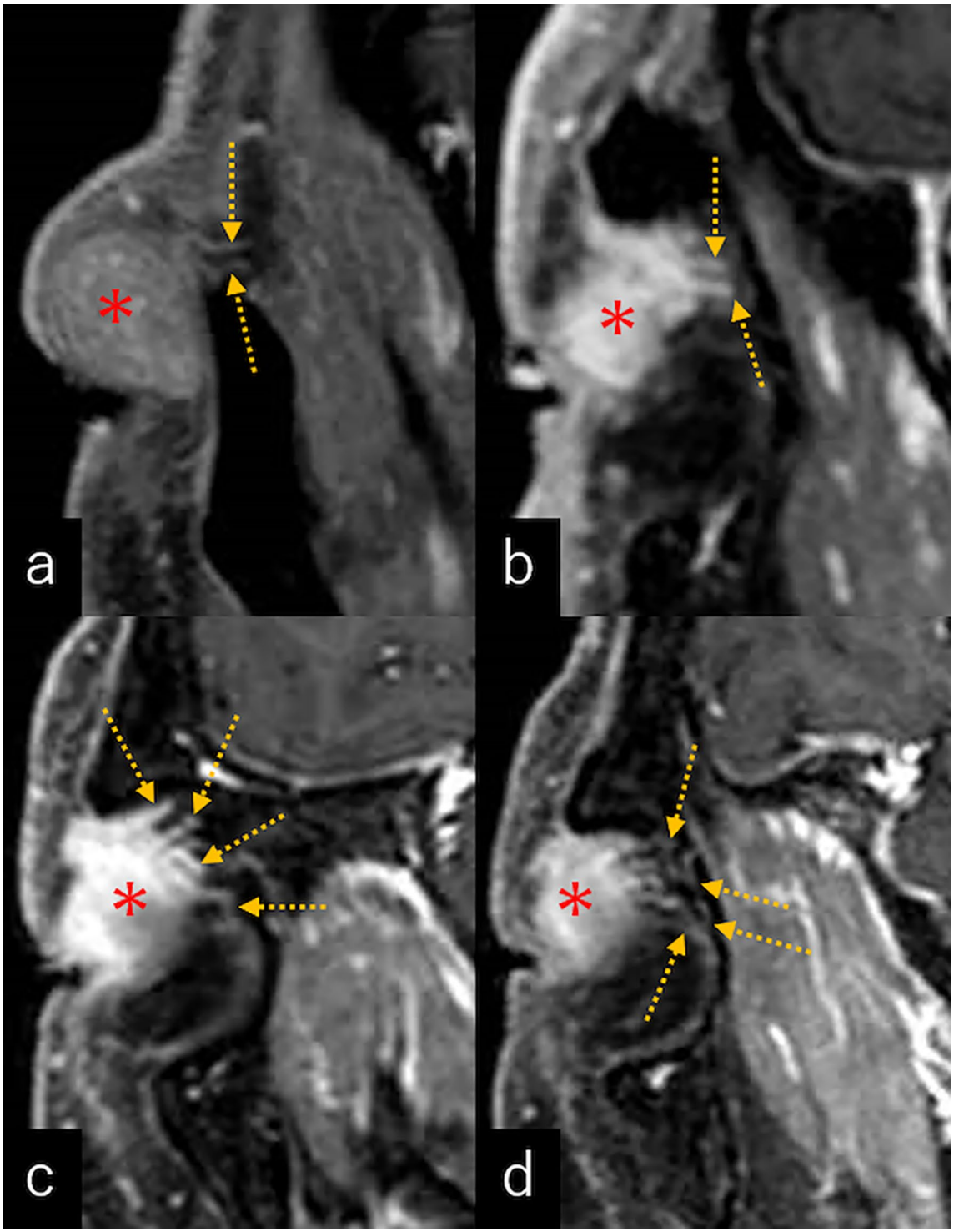

Fig. 2 Contrast-enhanced sagittal magnetic resonance images of three patients showing variable vessels arising from the lacrimal glands on the right (**a**, dashed arrows), left (**b**, d ashed arrows), and both sides (**c**, **d**, dashed arrows). Asterisk: lacrimal gland. **c**: right side, **d**: left side

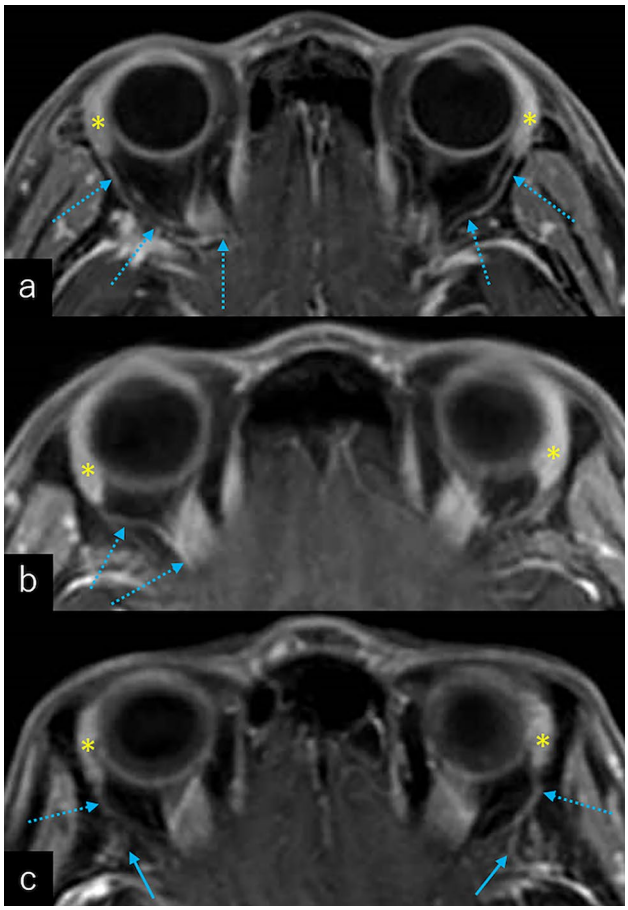

Fig. 3 Contrast-enhanced axial magnetic resonance images of different patients showing the lacrimal veins (LVs; (**a**–**c**), dashed arrows) with three distinct courses. **a** LV connecting to the superolateral cavernous sinus, **b** LV connecting to the superior ophthalmic vein, **c** LV connecting to the diploic channels of the greater wing of the sphenoid bone Asterisk: lacrimal gland

courses can contribute to performing function-preserving, safe maneuvers around the LG. Given the intraorbital location and shape of the LGs, sagittal images seemed suitable for delineating the LGs and the LV segments arising from them. However, to our knowledge, no study has explored LGs using sagittal MRI [3, 4, 9, 24, 27]. According to Lee et al. the mean LG width measured on an axial CT was small, being 4.1 mm on the right orbit and 4.3 mm on the left, while that on a coronal CT was 3.6 mm on the right and 3.8 mm on the left [14]. These findings may partly explain why LG data obtained from sagittal MRIs are scant. The present study adopted seamless scanning with a 1-mm slice thickness, which enabled the delineation of the LGs and LVs on sagittal images.

In the present study, laterality or sex differences were not statistically significant between the LD and SD groups. Furthermore, no specific age range was associated with a longer LD or SD. Conversely, a previous investigation using MRI showed that the thickness and area of the LGs decreased with age in women but not in men [27]. The methodology for measuring the LDs and SDs might have influenced the differences because LGs with variable shapes and dimensions are apparently not involved in a sagittal image. Further investigations are required to validate our results.

The present study had several limitations. First, the cohort comprised participants of heterogeneous age and sex. The participants were retrospectively evaluated and not randomly assigned to the MRI examinations. The LVs were assessed only on contrast-enhanced MRI and a small number of donated bodies to science, and the flow patterns of the veins were not assessed. At the present time, we cannot present a rationale for the three different LV types, identified in this study, based on the embryology. Furthermore, on the sagittal images, the LVs were not

Table 3 Classification of the identified courses of the lacrimal veins

	Connecting to the superolateral CS	Connecting to the SOV	Connecting to the DCs of the GW
Right	8	10	0
Left	5	6	1
Right and left	34	6	6
Total	47/76 (62%)	22/76 (29%)	7/76 (9%)

CS cavernous sinus, *DC* diploic channel, *GW* greater wing, *SOV* superior ophthalmic vein

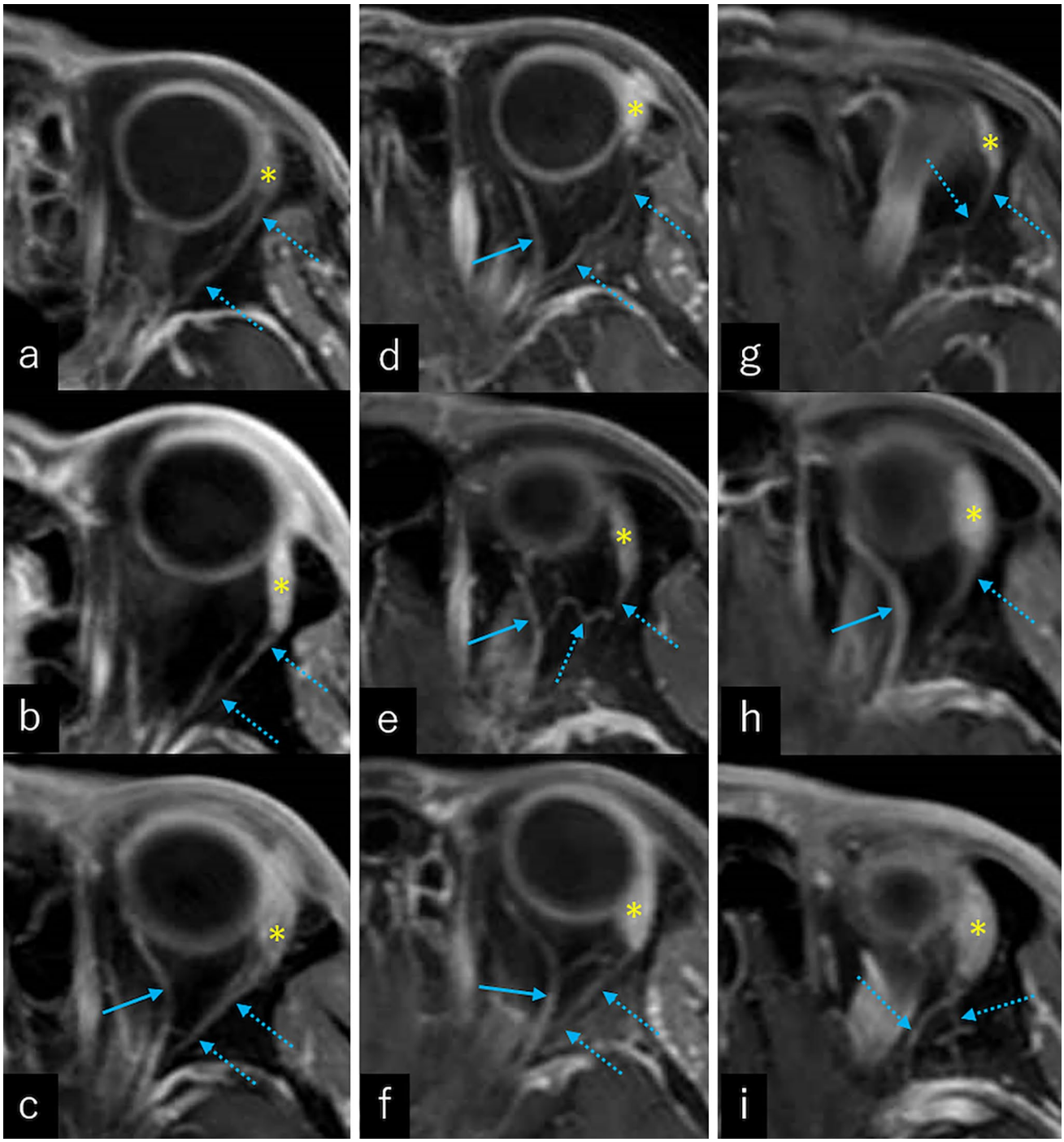

Fig. 4 Contrast-enhanced axial magnetic resonance images of different patients showing the left lacrimal veins (LVs) with variable courses. (**a**–**c**) LV connecting to the superolateral cavernous sinus, (**d**–**f**) LV connecting to the superior ophthalmic vein, (**g**–**i**) LV connecting to the diploic channels of the greater wing of the sphenoid bone Asterisk: lacrimal gland

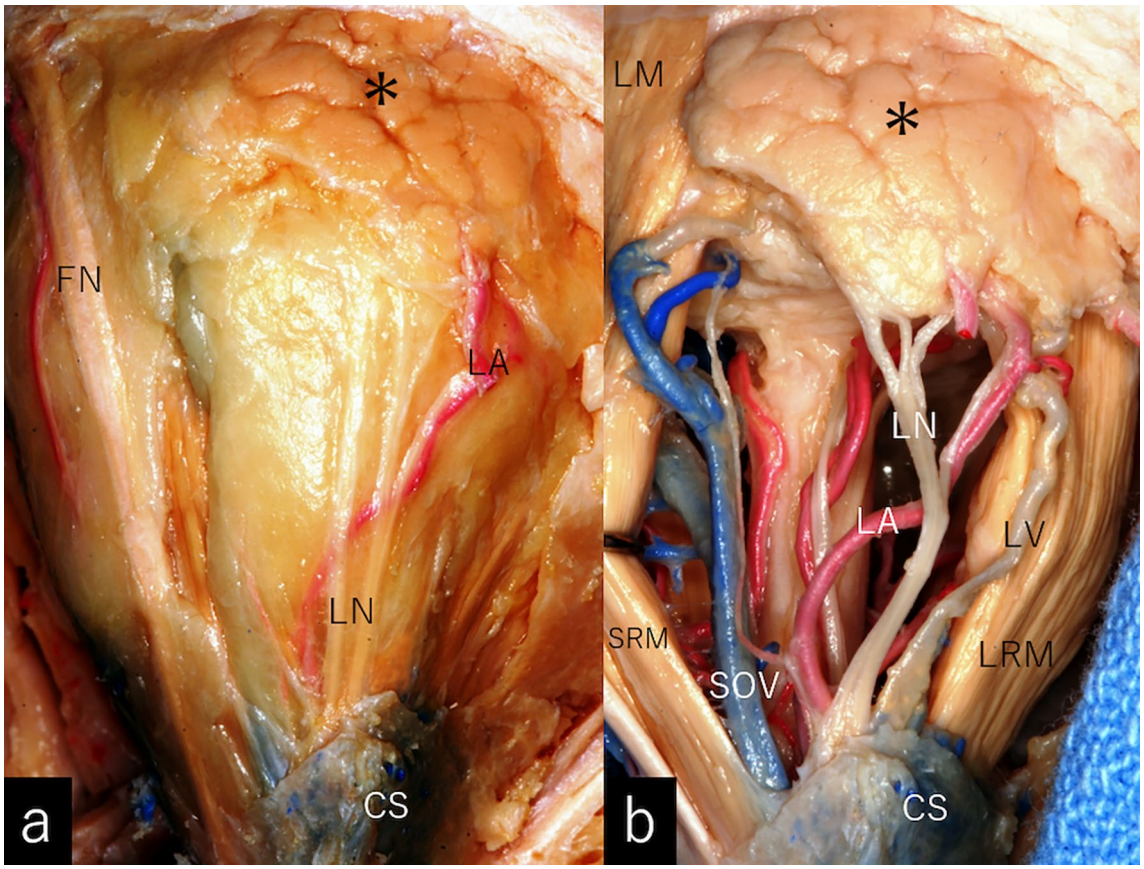

Fig. 5 Posterior and superolateral view of the right orbit on a donated body to science, after the removal of the orbital roof and its underlying periorbita (**a**) and after the removal of the orbital fat (**b**), revealing the lacrimal vein (LV) coursing between the posterior margin of the lacrimal gland (asterisk) and superolateral part of the cavernous sinus (CS), above the upper margin of the lateral rectus muscle (LRM). *FN* frontal nerve, *LA* lacrimal artery, *LM* levator muscle, *LN* lacrimal nerve, *SOV* superior ophthalmic vein, *SRM* superior rectus muscle

discriminated from the LAs for low performance in depicting more posterior courses. Despite these limitations, we believe that our results may improve our understanding of the LVs and LGs.

Conclusions

The LV may consistently emerge from the upper posterior margin of the LG. It commonly pours into the SOV or superolateral part of the CS.

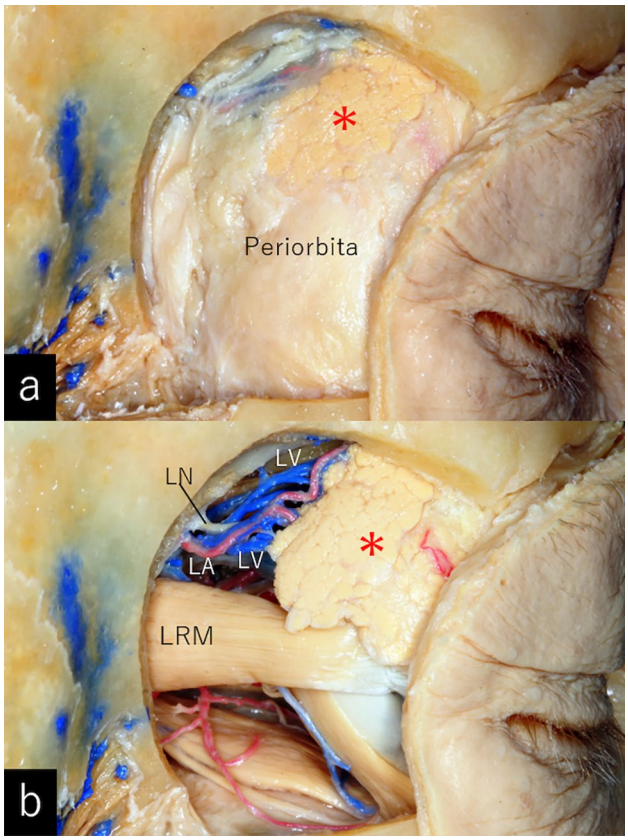

Fig. 6 Lateral view of a donated body to science, after a lateral orbitotomy (**a**) and removal of the periorbita and orbital fat (**b**), revealing all lacrimal veins (LVs) emerging from the posterior margin of the lacrimal gland (asterisk) and coursing superficially in the posterior direction along the course of the lacrimal artery (LA). *LN* lacrimal nerve, *LRM* lateral rectus muscle

Author contributions ST conceived the study, performed cadaver dissection, and wrote the manuscript, NS and HU collected the imaging data, ST and HI analyzed the imaging data.

Funding No funding was received for this study.

Data availability The data and materials used in this study are available from the corresponding author on reasonable request (Satoshi Tsutsumi).

Declarations

Conflict of interest The authors declare no conflicts of interest of a financial or personal nature.

Ethical approval All procedures in this study were performed in accordance with the ethical standards of an institutional and/or national research committee, as well as the 1964 Declaration of Helsinki and its later amendments or comparable ethical standards.

Informed consent Written informed consent was obtained from all participants included in the study for their participation and for the publication of the article.

References

1. Adawi MM, Abdelbaky AM (2015) Validity of the lateral supraorbital approach as a minimally invasive corridor for orbital lesions. World Neurosurg 84:766–771
2. Bilgili Y, Taner P, Unal B, Simsir I, Kara SA, Bayram M, Alicioglu B (2005) Doppler sonography of the normal lacrimal gland. J Clin Ultrasound 33:123–126
3. Buch K, Watanabe M, Elias EJ, Liao JH, Jara H, Nadgir RN, Saito N, Steinberg MH, Sakai O (2014) Quantitative magnetic resonance imaging analysis of the lacrimal gland in sickle cell disease. J Comput Assist Tomogr 38:674–680
4. Bukhari AA, Basheer NA, Joharjy HI (2014) Age, gender, and interracial variability of normal lacrimal gland volume using MRI. Ophthalmic Plast Reconstr Surg 30:388–391
5. Ducasse A, Delattre JF, Flament JB, Hureau J (1984) The arteries of the lacrimal gland. Anat Clin 6:287–293
6. Fiedor P, Ptasińska-Urbańska M, Makomaska-Szaroszyk E (1989) Variability of arterial vascularization of the human lacrimal gland. Folia Morphol (Warsz) 48:143–146
7. Gündüz K, Shields CL, Günalp I, Shields JA (2003) Magnetic resonance imaging of unilateral lacrimal gland lesions. Graefes Arch Clin Exp Ophthalmol 241:907–913
8. Hayek G, Mercier P, Fourier HD (2006) Anatomy of the orbit and its surgical approach. Adv Tech Stand Neurosurg 31:35–71
9. Hu H, Xu XQ, Wu FY, Chen HH, Su GY, Shen J, Hong XN, Shi HB (2016) Diagnosis and stage of Graves' ophthalmopathy: Efficacy of quantitative measurements of the lacrimal gland based on 3-T magnetic resonance imaging. Exp Ther Med 12:725–729
10. Izumi M, Eguchi K, Uetani M, Nakamura H, Takagi Y, Hayashi K, Nakamura T (1998) MR features of the lacrimal gland in Sjögren's syndrome. AJR Am J Roentgenol 170:1661–1666
11. Kanari H, Kagami SI, Kashiwakura D, Oya Y, Furuta S, Suto A, Suzuki K, Hirose K, Watanabe N, Okamoto Y, Yamamoto S, Iwamoto I, Nakajima H (2010) Role of Th2 cells in IgG4-related lacrimal gland enlargement. Int Arch Allergy Immunol 152:47–53
12. Kim JS, Liss J (2021) Masses of the lacrimal gland: evaluation and treatment. J Neurol Surg B Skull Base 82:100–106
13. Lee CS, Shim JW, Yoon JS, Lee SC (2012) Acute lymphoblastic leukemia presenting as serous macular detachment and lacrimal gland enlargement. Can J Ophthalmol 47:e33–e35
14. Lee JS, Lee H, Kim JW, Chang M, Park M, Baek S (2013) Computed tomographic dimensions of the lacrimal gland in healthy orbit. J Craniofac Surg 24:712–715
15. Lorber M, Vidić B (2009) Measurements of lacrimal glands from cadavers, with descriptions of typical glands and three gross variants. Orbit 28:137–146
16. Mergen B, Arici C, Kizilkilic O, Tanriover N, Kadioglu P (2021) Lacrimal gland enlargement and tear film changes in acromegaly patients: a controlled study. Growth Horm IGF Res 59:101397
17. Ogata H (2006) Anatomy and histopathology of the human lacrimal gland. Cornea 25:S82–S89
18. Rana K, Juniat V, Patel S, Selva D. (2022) Normative lacrimal gland dimensions by magnetic resonance imaging in an Australian cohort. Orbit https://doi.org/10.1080/01676830.2022.20
19. Seifert P, Spitznas M, Koch F, Cusumano A (1993) The architecture of human accessory lacrimal glands. Ger J Ophthalmol 2:444–454
20. Singh S, Basu S (2020) The human lacrimal: historical perspective, current understanding, and recent advances. Curr Eye Res 45:1188–1198
21. Singh S, Shanbhag SS, Basu S (2021) Palpebral lobe of the human lacrimal gland: morphometric analysis in normal versus dry eyes. Br J Ophthalmol 105:1352–1357

22. Stewart WB, Krohel GB, Wright JE (1979) Lacrimal gland and fossa lesions: an approach to diagnosis and management. Ophthalmology 86:886–895
23. Tamboli DA, Harris MA, Hogg JP, Realini T, Sivak-Callcott JA (2011) Computed tomography dimensions of the lacrimal gland in normal caucasian orbits. Ophthalmic Plast Reconstr Surg 27:453–456
24. Tenzel PA, Moffa D, Decilveo AP, Reddy HS (2019) Normal lacrimal gland volumes by magnetic resonance imaging and the relationship of lacrimal gland volume to orbital size. J Craniofac Surg 30:e741–e743
25. Tripathi BJ, Tripathi RC (1990) Evidence for the neuroectodermal origin of the human lacrimal gland. Invest Ophthalmol Vis Sci 31:393–395
26. Tucker SM, Lambert RW (1998) Vascular anatomy of the lacrimal gland. Ophthalmic Plast Reconstr Surg 14:235–238
27. Ueno H, Ariji E, Izumi M, Uetani M, Hayashi K, Nakamura T (1996) MR imaging of the lacrimal gland. age-related and gender-dependent changes in size and structure. Acta Radiol 37:714–719
28. Wu D, Zhu H, Hong S, Li B, Zou M, Ma X, Zhao X, Wan P, Yang Z, Li Y, Xiao H (2021) Utility of multi-parametric quantitative magnetic resonance imaging of the lacrimal gland for diagnosing and staging Graves' ophthalmopathy. Eur J Radiol 141:109815